INNER RADIATION BELT REPRESENTATION OF THE ENERGETIC ELECTRON ENVIRONMENT: MODEL AND DATA SYNTHESIS USING THE SALAMMBO RADIATION BELT TRANSPORT CODE AND LOS ALAMOS GEOSYNCHRONOUS AND GPS ENERGETIC PARTICLE DATA

R. H. W. Friedel
Los Alamos National Laboratory, Los Alamos, NM, USA

S. Bourdarie
ONERA/DESP, Toulouse, France

J. Fennell
The Aerospace Corporation

S. Kanekal
Catholic University of America

T. E. Cayton
Los Alamos National Laboratory

Abstract

The highly energetic electron environment in the inner magnetosphere (GEO inward) has received a lot of research attention in resent years, as the dynamics of relativistic electron acceleration and transport are not yet fully understood. These electrons can cause deep dielectric charging in any space hardware in the MEO to GEO region. We use a new and novel approach to obtain a global representation of the inner magnetospheric energetic electron environment, which can reproduce the absolute environment (flux) for any spacecraft orbit in that region to within a factor of 2 for the energy range of 100 KeV to 5 MeV electrons, for any levels of magnetospheric activity. We combine the extensive set of inner magnetospheric energetic electron observations available at Los Alamos with the physics based Salammbo transport code, using the data assimilation technique of ”nudging”. This in effect input in-situ data into the code and allows the diffusion mechanisms in the code to interpolate the data into regions and times of no data availability. We present here details of the methods used, both in the data assimilation process and in the necessary inter-calibration of the input data used. We will present sample runs of the model/data code and compare the results to test spacecraft data not used in the data assimilation process.

Introduction

The natural energetic electron environment in the Earth’s radiation belts is of general importance as dynamic variations in this environment can impact space hardware in those regions and contribute significantly to background signals in a range of other instruments flown in that region.

The interest in these events arises in part because of the increasing evidence of the correlation between the occurrence of these fluxes and of subsequent spacecraft operating anomalies or failures, especially at geosynchronous altitude. The prediction and mitigation of these effects should be possible when the causes of the flux buildups are under-stood [*Baker*, 1996]. In addition, because of the apparent complexity of these mechanisms, their understanding will contribute significantly to the general knowledge of transport and heating processes in the magnetosphere.

There is intense interest in isolating and understanding the mechanisms that contribute to the frequently observed MeV electron flux buildups in the outer magnetosphere, which is frequently observed during the recovery phase of geomagnetic storms.

While this is not a new topic, the unprecedented density of observations of relativistic electrons in the inner magnetosphere in the modern era has led to new questions and unsolved problems. In a recent review, *Friedel et al.* [2002] covers in detail the current state of research into this topic.

The scientific community is engaged in understanding the underlying physics to the observed dynamics; however, the question that is of most importance to spacecraft operators that are faced with an anomaly on a spacecraft is: "Was my anomaly due to the environment?" To answer this question one needs to be able to accurately describe the environment at any point in the inner region, *even in the absence of in-situ measurements*.

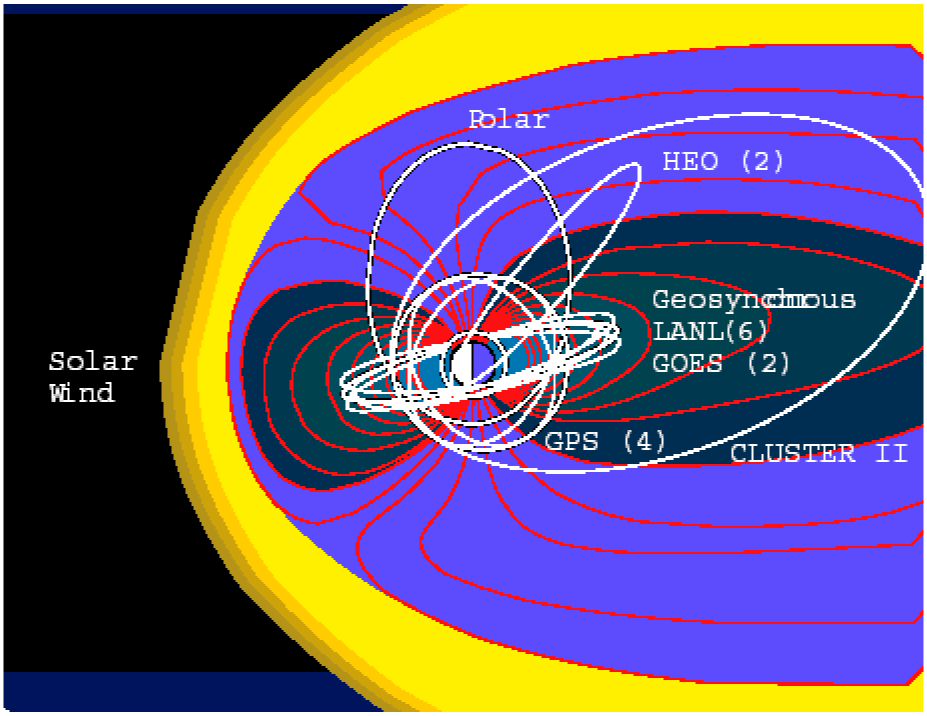

Figure 1. Schematic of current inner magnetosphere missions.

Data from any single point measurement in space has traditionally been used to derive information about the local environment at that satellite. There have been some earlier attempts of obtaining a dynamic global state of the inner magnetospheric electron populations based on single spacecraft observations *Friedel and Korth* [1995], based on the CRRES data, our community's last mission dedicated to the radiation belts. CRRES alone, on a 5.5 hour resolution, was able to provide a basically complete description of the inner region, across a wide eenergy range - due to it's ideally suited geosynchronous transfer orbit. However, CRRES flew in 1990/1991, and one has to look to other resources for such information today. *Friedel et al.* [1998] used a multi-spacecraft synthesis using simple interpolation techinque with data from up to 11 spacecraft to assemble a "map" of the inner radiation belt energetic electron population. This simple approach led to radiation belt maps that could represent the dynamics of the inner region on around a 3 hour time scale, but the simplistic interpolation and intercalibration scheme employed led to many unrealistic local time and radial variations which were clearly not physical but rather a reflection of insufficient instrument characterization.

In order to characterize this environment energetic particle detectors have routinely been flow on a range of DOE, NOAA and DOD spacecraft in geosynchronous, GPS and Moulniya orbits. Beyond these programmatic missions, this region has also been the subject of purely scientific investigations with current missions such as CLUSTER (ESA), POLAR (NASA). A schematic of the orbits of these missions available today is shown in Figure 1.

While the scientific measurements can provide the full three-dimensional particle distribution function and local magnetic field data (allowing data to be determined at constant adiabatic invariants, which are the coordinates that allow data to be inter-compared throughout the inner magnetosphere), these data are not available on long time scales or on a reliable basis into the future, and, when present, have a limited spatial coverage by themselves.

Data from the programmatic missions provides excellent time coverage, longevity and spatial coverage, but with particle instrumentation that provides omni-directional data and no magnetic field information.

The challenge is thus to utilize the available data in a framework that still allows us to retrieve high fidelity global maps of the inner radiation belts. Our approach here is a synthesis between multiple point space measurements and a physics based radiation belt model that makes full use of all the data from our current constellation of energetic electron measurements in space (up to 6 simultaneous geosynchronous and 4 simultaneous GPS orbit measurements) and uses the model to provide a physical interpolation between the data. The end result is a dynamic and global model of the energetic electron radiation environment at all points in space, which can provide reliable environmental data for locations of satellites that do not carry any energetic particle instrumentation.

Data for our assimilation at this point comes primarily from the LANL Geosynchronous ESP instrument [*Reeves et al.*, 1997]; the LANL GPS energetic particle sensors [*Feldman et al.*, 1985]. For testing purposes we also use data from the HEO energetic particle instruments [*Blake et al.*, 1997].

The Model

We use here a custom version of the SALAMMBO radiation belt code developed by our collaborators at ONERA in Toulouse, France [*Beutier and Boscher*, 1995; *Bourdarieet al.*, 1996b; *Boscher et al.*, 2000]. This is a diffusion code that models physical processes in the inner magnetosphere by their respective diffusion coefficients (radial and pitch angle diffusion). A schematic of this code is shown in Figure 2.

This code used the planetary disturbance index Kp to parameterize radial diffusion and the position of the plasmapause which controls wave activity and thus pitch angle diffusion. The code is symmetrical in local time since on a given drift orbit particle fluxes are the same at all local times on timescales on the order of the drift time, which is typically around 10 minutes for the highly energetic electrons. The code traces the full particle distribution function in the coordinate space of L* (magnetic coordinate of the drift shell), B/Bo (the ratio of the local magnetic field strength to the equatorial magnetic field strength on a given magnetic field line) pitch angle and energy.

The code has successfully been used to model the response of the inner magnetospheric energetic electron population to geomagnetic storms [*Bourdarie et al.*, 1996a]. Recent work by *Summers et al.* [1998] pointed out the importance of energy diffusion by whistler mode waves for relativistic electrons as being an important energization source, and *Meredith et al.* [2002] have shown a direct relation- ship between relativistic electron acceleration and substormenhanced whistler mode chorus. This physics is currently not included in the Salammbo code. As it turns out, our data assimilation can compensate for this: inclusion of relevant amounts of data "pulls" the code in the right direction, even in the absence of this missing physics.

Data preparation

In response to the lessons learned by *Friedel et al.* [1998] a large amount of effort was devoted processing our data to a level that made inclusion into a model feasible. Models in general have no way of distinguishing between "good" and "bad" data - garbage in simply leads to garbage out. early assimilation runs suffered from stability problems arising from importing data that was wildly different from the model representation. It was necessary to interpolate and clean up the data to a high degree of fidelity before any import of the data into the model was attempted. This effort alone took almost 4 Friedel et al. 2 years. Here we present a brief outline of the procedures adopted.

Inter-calibration

It was decided to boot-strap out data to the last high- fidelity energetic particle instrument flown in the inner magnetosphere, the MEA instrument [*Vampola et al.*, 1992] on board CRRES. This was a magnetic spectrometer with full anti-coincidence electronics that does not suffer some of the background and noise problem encountered on the LANL GEO, GPS and HEO instruments. Using the overlapping time periods between CRRES and LANL GEO and GPS missions, we could inter-calibrate those missions to agree with the CRRES measurements. This required the definition of conjunctions between two spacecraft. In order to obtain a sufficient number of conjunctions, we used the following set of conditions (see Figure 3).

- $L < 6$ and $\Delta L < 0.1$
- $\Delta B/D_{EQ} < 0.1$
- Magnetic local time (MLT) within 2 hours of 06:00 and 18:00 and $\Delta MLT < 0.15$
- Magnetospheric activity quiet ($Kp < 2$ for two days before conjunction
- $\Delta t < 3$ hours

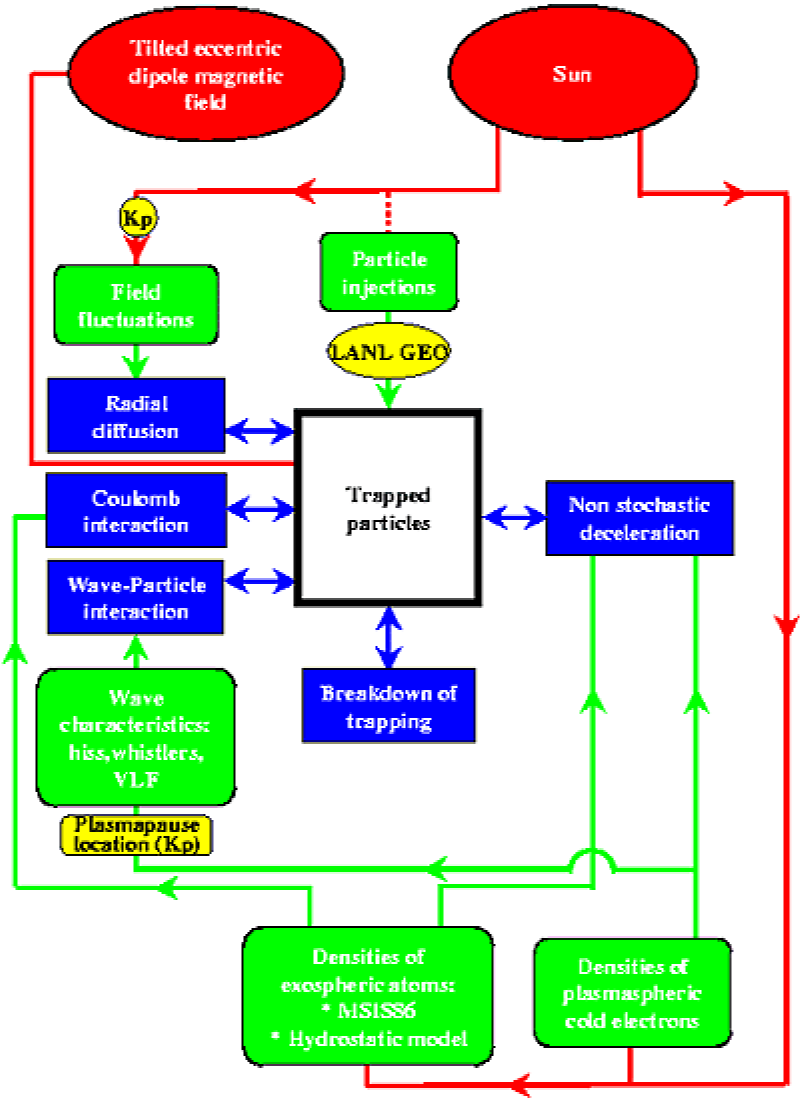

Figure 2. Schematic the Salammbo radiation belt code for Electrons

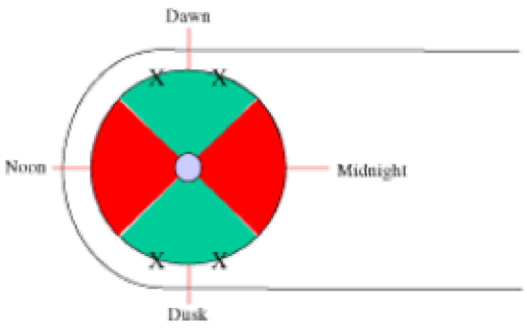

Figure 3. Schematic showing the green region of "allowed" Conjunctions

The restriction in local time is due to the use of model magnetic fields in obtaining the required model coordinates (L*), which are best in these regions. The low activity requirement allows us to relax the time constraint on conjunctions; this allows us to obtain more conjunction points.

Since GEO and GPS can never fulfill the conjunction requirements used here, they were both independently calibrated against CRRES, which has conjunctions with both.

Figure 4 shows our resulting inter-calibration between LANL geosynchronous and CRRES data, showing an excellent match. Figure 5 shows the result of inter-calibrating CRRES with GPS ns18. For the GPS spacecraft, the energy thresholds are gain dependent; the red triangles show the raw, uncorrected data and the black crosses the new spectra after adjusting the energy thresholds to match the CRRES spectra.

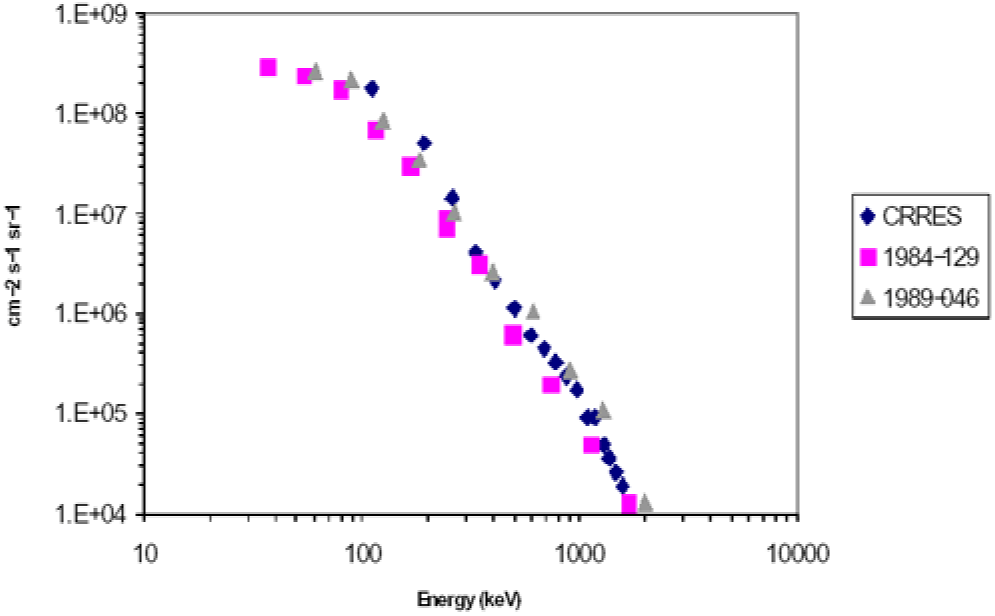

Figure 4. Matching spectra between CRRES and two LANL GEO spacecraft in September 1990

Once these calibrations had been done the calibrations were propagated forward in time by matching overlapping Data assimilation with the Salammbo code 5 GEO and GPS data. In this way a consistent set of intercalibration data for all GPS and GEO spacecraft could be found to the present. Our best estimate of the accuracy of this intercalibration is that on average the calibration is good to within a factor of 2.

The details of this calibration procedure can be found in a 60-page document available at http://nis-www.lanl.gov/friedel/lws_proj/GPS_calibration_2002.doc.

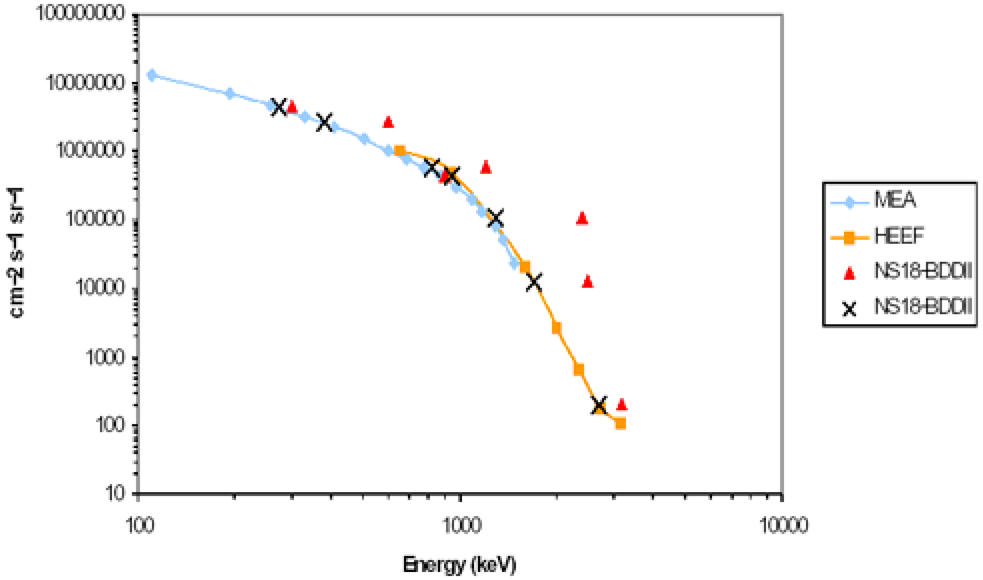

Figure 5. Matching spectra between CRRES and GPS ns18 spacecraft in September 1991

Data contamination

It is well known that during times of solar energetic proton events (SEPs) many of the detectors used here are contaminated with strong background counts. We use the NOAA GOES energetic proton data to mask out our data during such active times, by monitoring a threshold flux of $10^{-5}cm^{-1}s^{-1}sr^{-1}keV^{-1}$ on the 39–65 MeV proton channel. During times when this threshold is exceeded we to not assimilate any data into out model but allow the model to run freely.

Saturation / background

Data saturation occurs in some instruments as a limit of counting speed during high count intervals, leading to an artificial plateau in observed counts. These levels are statistically observable and we can ensure that only those data below saturation levels are used in the assimilation process.

Background levels due to thermal noise or other contamination such as cosmic rays are present in all particle instruments. These levels can be detected by examining data during intervals when the spacecraft are outside the trapping region for energetic electrons, this occurs over the polar cap on open field lines for GPS and during extreme magnetospheric compression events for the geosynchronous regions. We detect and track these background counts over time and subtract these counts before using the data in our assimilation.

Data Assimilation Techniques

This model has been tightly integrated into our data system at LANL, and allows us to input data from various spacecraft sources directly into the model grid. The difference here is that the model no longer uses a simple boundary condition, but allows direct input into the code grid at any location for which data is available. This corresponds to the data assimilation method of ”nudging”.

Data input

In order to seed the code with real data the data has to be transformed into the model coordinate space. The Salammbo code internally uses a custom spaced grid in energy, pitch angle and L*. L* here corresponds to the third adiabatic invariant and is closely related to a particle’s drift shell. For energetic particles for which electric field drifts can be ignored, L* almost exactly labels the drift shell a real particle follows.

Due to the nature and limitations of the data used the determination of this mapping requires some assumptions:

- L* depends on a magnetic field model. At this stage of our assimilation work we use the same model for all data - the static Olson Pfizer 1977 model. Extensions to more complex and dynamic models are planned.
- Current data sources provide omni-directional data and no magnetic field information. We thus use a statistical representation of pitch angle distributions as a function of L* derived from CRRES data. This is overwritten at times when we are able to determine the pitch angle distribution directly from data (see Figure 6): whenever there are ”conjunctions” in the input data (satellites at the same L* but at different magnetic latitudes) we use a fitting procedure to derive the best fit to a pitch angle distribution that yields the observed omni-direction data at the two latitudes. Such “measured” pitch angle distributions override the statistical distributions with a persistence of one hour.
- Energy channels are interpolated to the required grid energy values. Measurements are assigned to the two closest grid points in L weighted according to their distance from the grid point, to ensure smooth data insertion.
- The outer boundary of the simulation is at L*=9. The value of this boundary is either set the AE8 model 6 Friedel et al. value at L=9 [*Vette*, 1991] or when GEO data is available to the geosynchronous data values adiabatically shifted to L*=9.

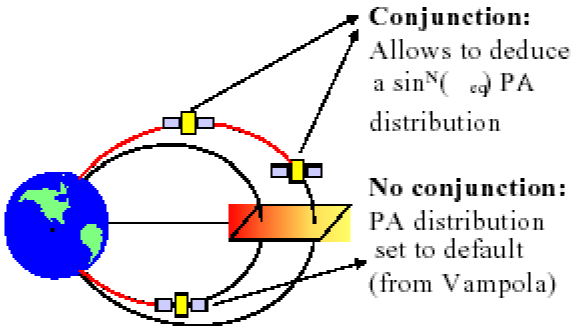

Figure 6. Schematic of model "conjunctions" allowing determination of pitch angle distribution from omni-directional data.

We need to point out here that the methods described here represent out first approach and are constantly being re-fined. As the model evolves (finer grid spacing) and our data evolves (inclusion of pitch angle sorted data from LANL GEO, POLAR and CLUSTER) our assimilation techniques will become more complex.

In a general run input data thus transformed is entered into the grid for the locations and times available, and the model is allowed to act for all other periods and locations.

Model output

The output of the Salammbo code is a time series of states in model coordinates that define the global inner radiation belt for energetic electrons in L* (1.1 to 8). The time resolution currently is 10 seconds.

Once a model run for a given set of input data for a given period has been performed, we can ”fly” any required spacecraft orbit through the model grid. All we need to do is to transform any satellite ephemeris to the required magnetic coordinates of the model grid and specify which energy we want. The model can return data either in differential or integral energy flux, either pitch angle resolved or summed to give an omni-directional equivalent.

First Results

An initial run was performed for the period of one of the NSF GEM storm of September 1 - October 10, 1998. The model was run with the correct Kp values for this period, and data was assimilated into the model from one geosynchronous satellite (LANL-GEO 1994 084) and one GPS satellite (ns33). The model output at one time step is shown in Figure 7.

In order to assess model performance we used several test satellites that were "flown" through the model results. We then compared the model fluxes versus the actually measured fluxes on the test satellites.

Model + LANL GEO, HEO as test

Here we performed ouR model run using ONLY the LANL GEO data as input. The results are shown in Figure 8. The model is initialized with a default state at the beginning of the run representing an average quiet magnetosphere, taken from CRRES measurements.

HEO data is used as a test: At this point HEO HAS NOT been fully inter-calibrated with GEO and GPS. Initial com- parisons however show that for the energy range chosen in our comparisons here, agreement between HEO, GPS and GEO is generally good.

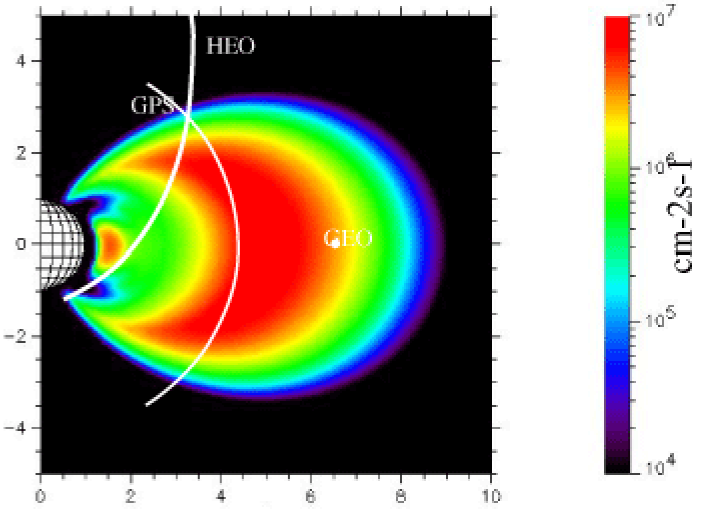

Figure 7. A graphical representation of the model fluxes at one time step in the simulation. Shown superimposed are the orbits of lANL GEO and GPS and HEO (used for testing output only)

The description of Figure 8 also applies to Figures 9 and 10. The top three panel show data in the L* versus time format, where each color coded vertical bar in the plot represents the flux along the satellites cut through L at this time. The top panel shows the actual HEO-2 satellite data for the ¿0.63 MeV channel. The next panel shows the model output along the orbit on HE0-2; both these panels share the same color bar. The third panel shows the ratio model divided by data, and the color bar represents ratios up to 10 in yellow/ red graduations and ratios down to 0.1 in blue/dark blue graduations. The bottom panel shows the Dst storm index for reference.

Ideally, if model and data agree 100 %, this ratio should be 1 (black). Here we see large deviations from 1 in two areas: the outer belts near GEO and the inner region near the slot. The first discrepancy can be explained in terms of the missing model physics as described earlier: whistler chorus interactions are not yet modeled, and in the absence of any assimilation data inside of geosynchronous that helps define the GEO pitch angle distributions. HEO has a highly elliptical orbit and cuts through GEO at high latitude – obviously the statistical pitch angle representation is not a good one for this time period. The discrepancy at low L is simply due to wrong initial state and short model run: diffusion is extremely slow in this region and we simply observe a persistence of the initial state.

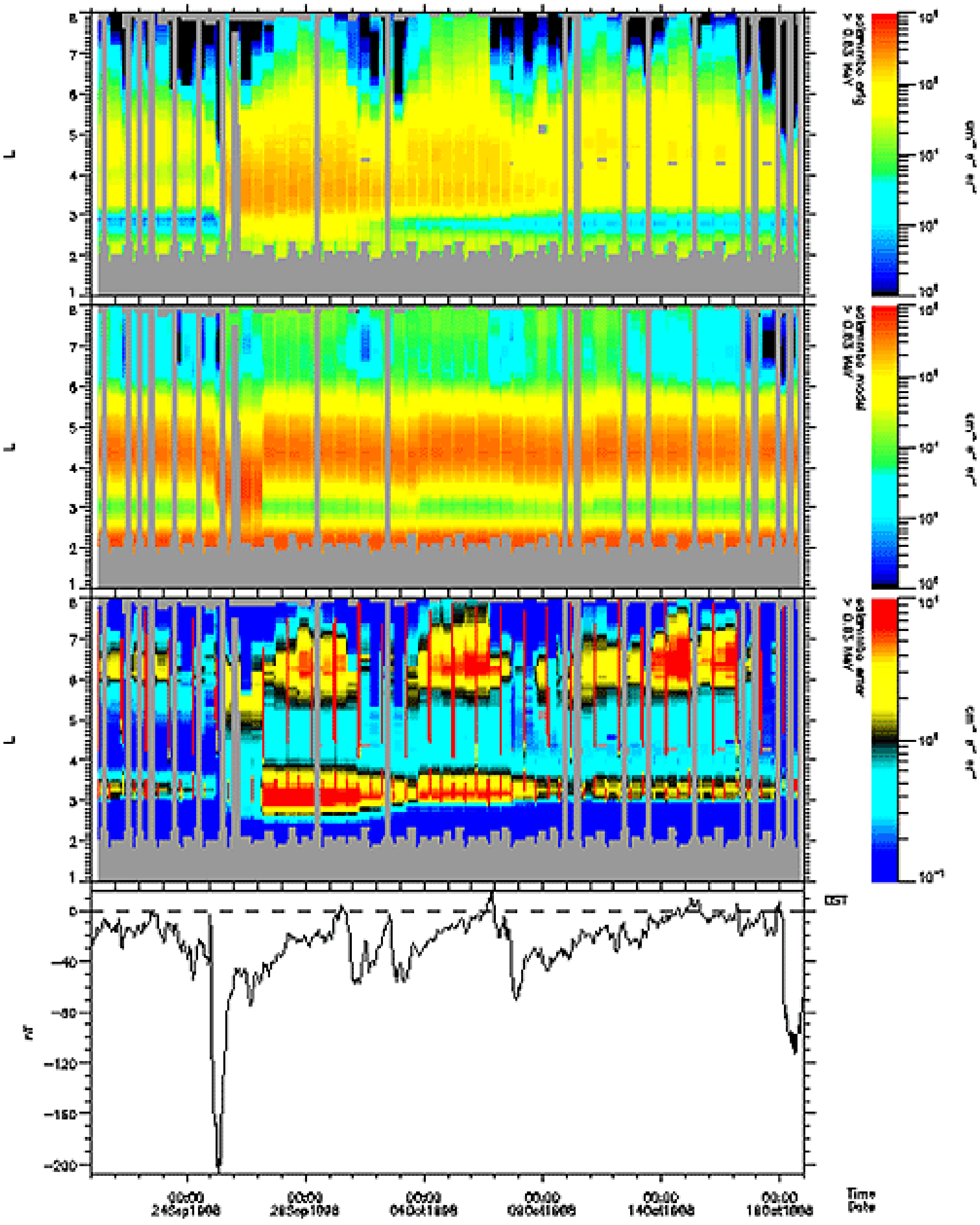

Figure 8. Data, model and comparison outputs. See text for details.

Model + LANL GEO + GPS, HEO as test

This model run uses both the LANL GEO and GPS data as input, which assimilates data into the region down to L=4. The results are shown in Figure 9.

As a quick visual comparison between Figures 8 and 9 easily shows the model performance is much improved by the inclusion of just one additional satellite in the assimilation process. This is particularly true for the region which is now covered by data input - GPS data is available from L=4 outward, and in that region the model /data comparison shown mainly black and light yellow indicating performance of model to within a factor of 2-3 of the data. Inclusion of GPS around L=4 to 5 compensates for the missing physcis in the region, while near geo it helps to properly define the pitch angle distribution which is needed to correctly estimate the fluxes at the high latitudes of HEO. The inner region remains badly represented here since no additional satellite data was used there. The addition of low altitude data from SAMPEX will help out in this region.

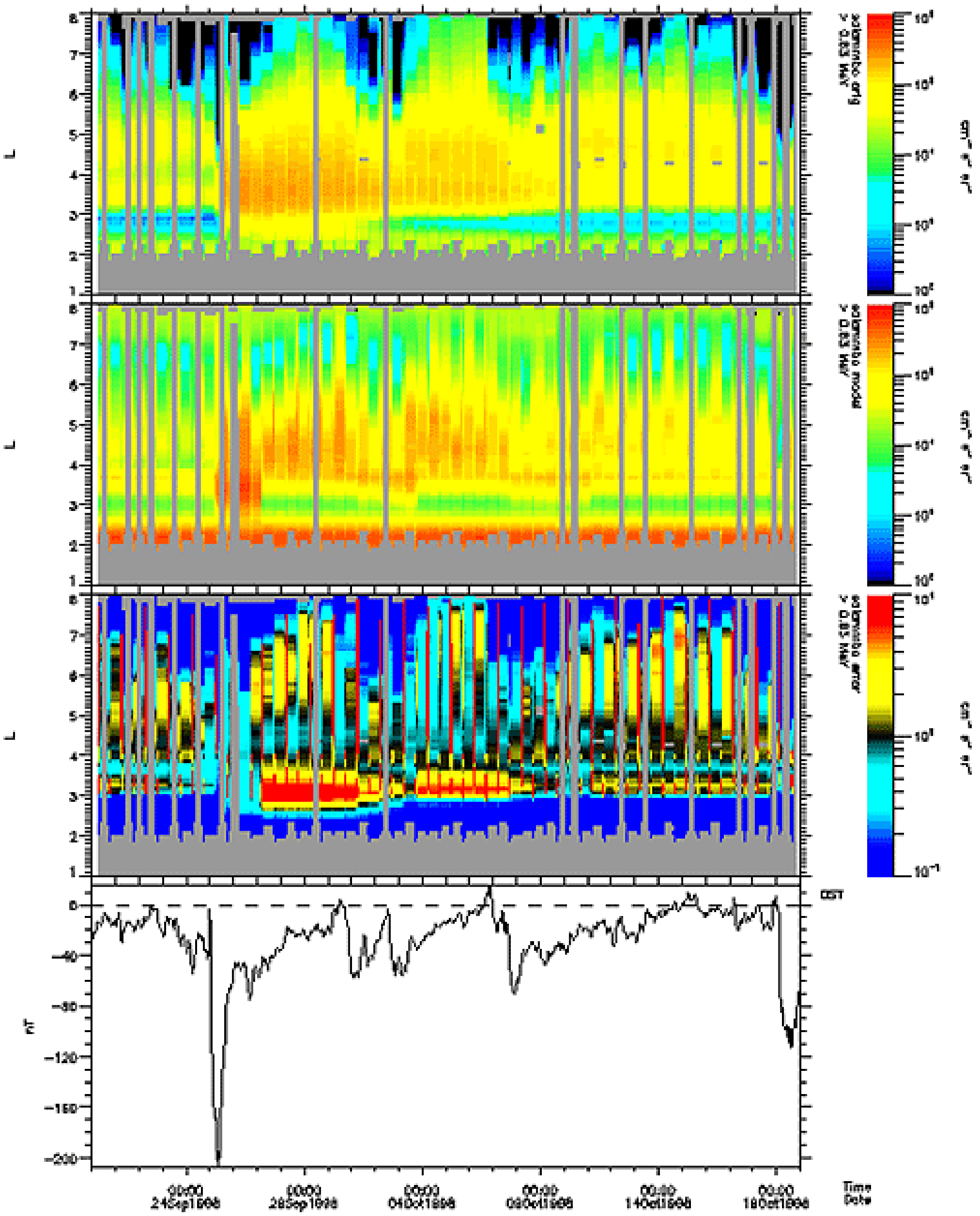

Figure 9. Data, model and comparison outputs. See text for details.

Model + LANL GEO + GPS, another GPS as test

This model run uses both the LANL GEO and GPS ns33 data as input, but uses another GPS satellite, ns24 as the test satellite. The results are shown in Figure 10.

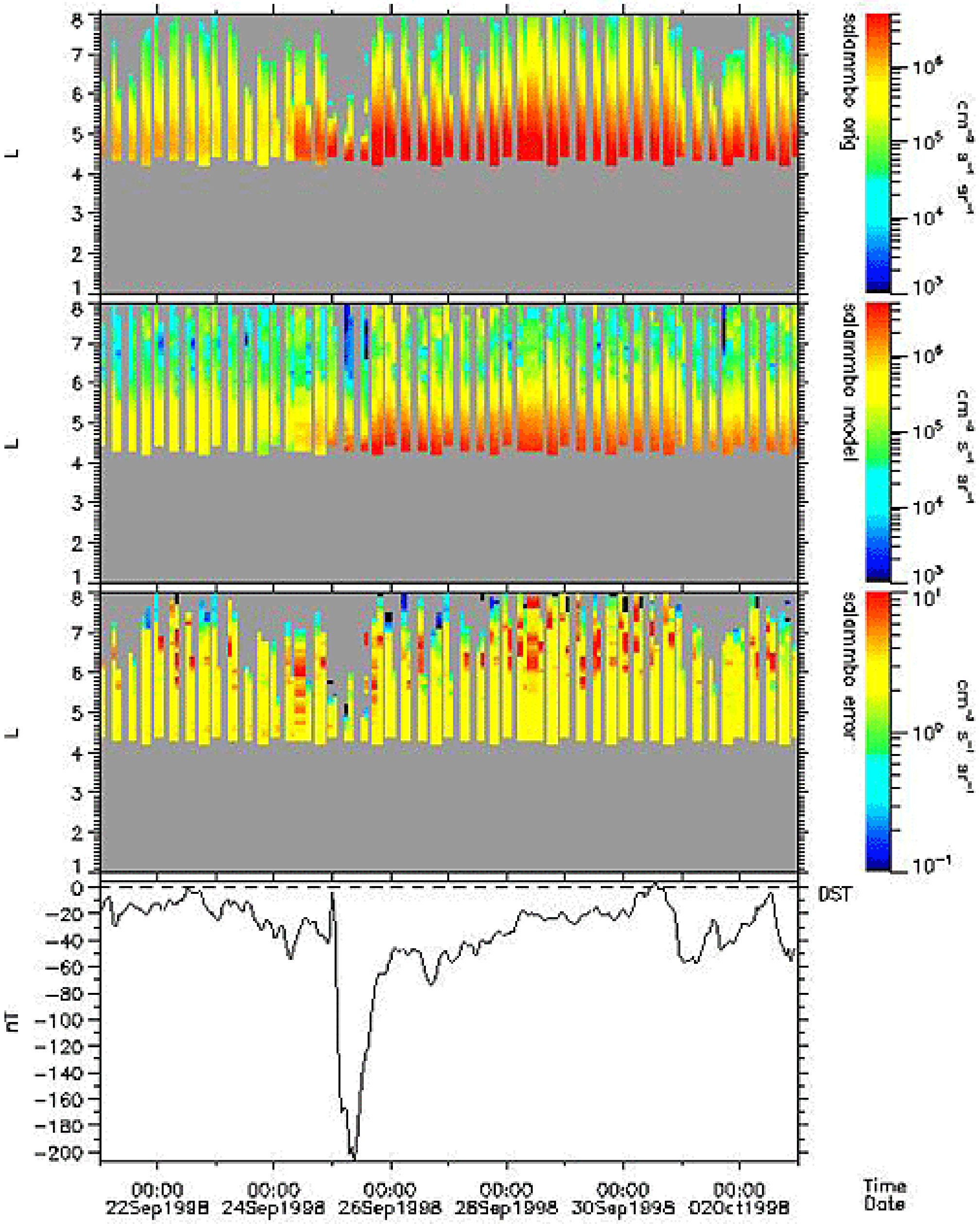

Figure 10. Data, model and comparison outputs. See text for details.

Not surprisingly the model data comparison shows consistent ratios of 2-3 throughout the whole period, regardless of activity levels. This is expected as the region tested is also the region seeded with assimilation data. What the residual ratios of 2-3 however indicate is that this is about as good as we can hope to get with this method. Factors of 2-3 represent the fidelity of our original data intercalibration.

Summary

This project is in its initial stages and a lot of further fine tuning of the assimilation method and input data is needed. First results however are promising. We are confident that for spacecraft orbits in the MEO to GEO orbital range we can reproduce the real environment with this method to 10 Friedel et al. within factors of 2-3.

We will extend our model further to include as many data sources as possible, especially at lower altitudes. It must be noted that before further data can be incorporated a similar intercalibration effort as done fro GEO and GPS needs to be undertaken for HEO, POLAR, SAMPEX and CLUSTER. Further, once pitch angle resolved input data is being used from GEO, POLAR and Cluster our data assimilation methods need to be upgraded to correctly map the data into the model, as shell splitting effects in real magnetic fields need to be taken into account.

We anticipate using this model/data synthesis both for research and for Space Weather now-casting (limited by realtime data availability, currently not possible for GPS). For research, having this model ”specify” the real environment we can then run the model in a not assimilative mode to see what physics is missing/under-represented. For Space Weather, we can specify the environment for any past time time going back approximately one solar cycle, which is required for any post-event anomaly analysis.

Further, we can use this model to explore exactly what kinds of data and data locations are needed for optimal input that would increase the fidelity of the model.

Acknowledgments.

We thank R. D. Belian, R. A. Christensen, and M. M. Meier for providing assistance with the LANL satellite data,W. Feldman and C. Ingraham for the GPS data. This work was supported by grant # W-19,957 from NASA’s LWS (Living with a Star) Research and Technology Program and from the US Department of Energy Office of Basic Energy Science (OBES).

References

1. Baker, D. N., Solar wind-magnetosphere drivers of space weather, J. Atmos. Terr. Phys., 58, 1509–1525, 1996.

2. Beutier, T., and D. Boscher, A three-dimensional analysis of the electron radiation belt by the salammbˆo code, J. Geophys. Res., 100, 14,853–14,861, 1995.

3. Blake, J. B., D. N. Baker, N. Turner, K. W. Ogilvie, and R. P. Lepping, Correlation of changes in the outer-zone relativisticelectron population with upstream solar wind and magnetic field measurements, Geophys. Res. Lett., 24, 927–929, 1997.

4. Boscher, D., S. Bourdarie, R. M. Thorne, and B. Abel, Influence of the wave characteristics on the electron radiation belt distribution, Adv. Space Res., 26 (#1), 163–166, 2000.

5. Bourdarie, S., D. Boscher, T. Beutier, J. A. Sauvaud, and M. Blanc, Magnetic storm modeling in the Earth's electron belt by the salammbo code, J. Geophys. Res., 101, 27,171–27,176, 1996a.

6. Bourdarie, S., D. Bosher, T. Beutier, J. A. Sauvaud, M. Blanc, and R. H. W. Friedel, A physics based model of the radiation belt flux at the day timescale, in Proceedings of the Symposium on Environment Modelling for Space-Based Applications, SP-392, pp. 159–163, ESA, ESA Publications Division, ESTEC, Noordwijk, The Netherlands, 1996b.

7. Feldman, W.,W. Aiello, D. Drake, and M. Herrin, The BDD II: An improved electron dosimeter for the global positioning system, Tech. Rep. LA-10453-MS, Los Alamos Natl. Lab., Los Alamos, N. M., 1985.

8. Friedel, R. H.W., and A. Korth, Long-term observations of keV ion and electron variability in the outer radiation belt from CRRES, Geophys. Res. Lett., 22, 1853–1856, 1995.

9. Friedel, R. H. W., G. D. Reeves, and T. Obara, Relativistic electron dynamics in the inner magnetosphere – a review (online pdf version), J. Atmos. Terr. Phys., 64, 2002.

10. Friedel, R. H. W., et al., A multi-spacecraft synthesis of relativistic electrons in the inner magnetosphere using LANL, GOES, GPS, SAMPEX, HEO and POLAR, Adv. in Space Res., 1998.

11. Meredith, N., R. B. Horne, R. Iles, R. M. Thorne, D. Heyndericks, and R. A. Anderson, Outer zone relativistic electron acceleration associated with substorm-enhanced whistler mode chorus, J. Geophys. Res., 107, 1144–1144, 2002.

12. Reeves, G. D., R. D. Belian, T. C. Cayton, M. G. Henderson, R. A. Christensen, P. S. McLachlan, and J. C. Ingraham, Using Los Alamos geosynchronous energetic particle data in support of other missions, in Satellite-Ground Based Coordination SourceBook, edited by M. M.Lockwood and H.J.Opgenoorth, pp. 263–272, ESA Publications, ESTEC, Noordwijk, The

Netherlands,1997.

13. Summers, D., R. M. Thorne, and F. Xiao, Relativistic theory of wave-particle resonant diffusion with application to electron acceleration in the magnetosphere, J. Geophys. Res., 103, 20,487– 20,500, 1998.

14. Vampola, A. L., J. V. Osborne, and B. M. Johnson, CRRES magnetic electron spectrometer AFGL-701-5A (MEA), J. Spacecr.Rockets, 29, 592–594, 1992.

15. Vette, J. I., The NASA/National Space Science Data Center Trapped Radiation Environment Model Program (1964–1991), Tech. Rep. NSSDC/WDC-A-R & 91-26, Goddard Space Flight Center, NASA/GSFC, Greenbelt, USA, 1991.

16. R. H. W. Friedel, T. E. Cayton Los Alamos National Laboratory, P.O. Box 1663, Los Alamos, NM 87545 (tcayton@lanl.gov; rfriedel@lanl.gov) This preprint was prepared with AGU's LATEX macros v5.01, with the extension package 'AGU__' by P.W. Daly, version 1.6b from 1999/08/19.